Semi-Passive Three Axis Attitude Stabilization for Earth Observation Satellites using the Drag Maneuvering Device

Sanny Omar[1], Camilo Riano Rios[1], Riccardo Bevilacqua[1]

[1]University of Florida
939 Sweetwater Dr., Gainesville, Florida, United States
Phone: +1-352-846-1477, Mail: sanny.omar@gmail.com

Abstract: The rise of small satellites has led to many missions with simple attitude and orbit control requirements. For example, a small Earth imaging satellite may require keeping one face nadir pointing within 10 degrees while maintaining a slot in a low Earth orbit within ± 100 km. However, legacy attitude and orbit control techniques including reactions wheels and thrusters can easily cost hundreds of thousands of dollars and provide more control capability than is needed for such a mission.

This paper introduces the Drag Maneuvering Device (DMD) that could replace such systems on many missions and consists of four retractable tape spring booms deployed in a dart configuration. The DMD can actively modulate the drag area of the host satellite for orbital maneuvering and post-mission disposal while providing passive 3-axis attitude stability using aerodynamic and gravity gradient torques. Magnetorquers integrated into the DMD damp attitude oscillations and help ensure the satellite stabilizes with the correct face nadir pointing. An overview of the DMD design is provided in this paper and the results of the attitude and orbit simulations used to characterize the DMD performance and devise a control and operations methodology are detailed.

1. INTRODUCTION

Attitude and orbit control have been important considerations since the early days of space exploration [1]. Traditionally, attitude control has been performed using reaction wheels, control moment gyros, and thrusters, and orbit control has been performed using thrusters [2], [3]. These legacy attitude and orbit control systems have been complicated and expensive, but highly accurate and rapidly responding, making them well suited to large, high-budget satellite missions. Alternative attitude and orbit control methodologies using environmental forces and torques have been proposed [4] and have become particularly valuable in recent years with the introduction of small satellites such as CubeSats [5] that lack the volume, power, or budget for the legacy systems. Aerodynamic drag force is a naturally occurring effect that is dependent on the satellite's orientation, geometry, and orbital regime [4]. Aerodynamic drag has been utilized for orbital maneuvering, and methods for using aerodynamic torques for attitude control have been investigated in prior literature [6]. Gravity gradient torques are dependent on the spacecraft moments of inertia and can be harnessed for attitude stabilization through the use of a gravity gradient boom [3], [7]. In low Earth orbits, electromagnets (called magnetorquers) embedded in the satellite can interact with the Earth's magnetic field to impart torques on the satellite. Magnetorquers have commonly been used for detumble and for reaction wheel de-saturation [8]. These effects have been investigated for attitude control in prior literature, but prior solutions either do not provide 3-axis attitude control or require actuators like thrusters or wheels to provide complete control that is robust and reliable. Methods that do investigate 3-axis attitude control would require costly sensors to provide 3-axis attitude determinations. Techniques that use aerodynamic torques for ram-alignment [6], gravity gradient torques for zenith alignment [7], or magnetic torques for magnetic field alignment [9] all leave one axis of rotation unconstrained. To date, there is no device or control

solution to the authors' knowledge that facilitates aerodynamically based orbital maneuvering while enabling 3-axis attitude stabilization without the need for attitude determination.

This paper introduces the Drag Maneuvering Device (DMD) which provides such an attitude and orbit control solution. The theory, operations, and control methodology behind the DMD are discussed and a 6DOF high fidelity attitude and orbit model is introduced to validate the semi-passive 3-axis attitude stabilization of the DMD.

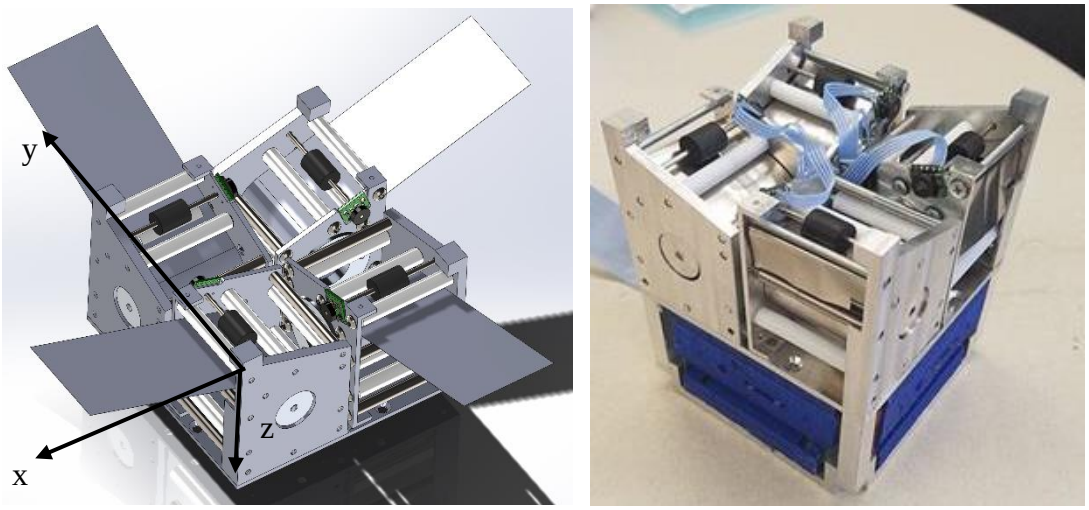

Figure 1. Drag Maneuvering Device (DMD) CAD model and Prototype

2. DRAG MANEUVERING DEVICE DESIGN

The Drag Maneuvering Device (DMD), formerly called the Drag DeOrbit Device (D3) [10], consists of four tape spring booms, each 3.7 m long and 4 cm wide, inclined at a 20 degree angle relative to the face of the satellite to which the DMD is attached as shown in Figure 1. The booms are deployed in this shuttlecock configuration to provide passive aerodynamic attitude stability. Additionally, one pair of opposing booms can be partially retracted while the other pair is fully deployed to create a clear minimum moment of inertia axis along the direction of the deployed booms. Gravity gradient torques

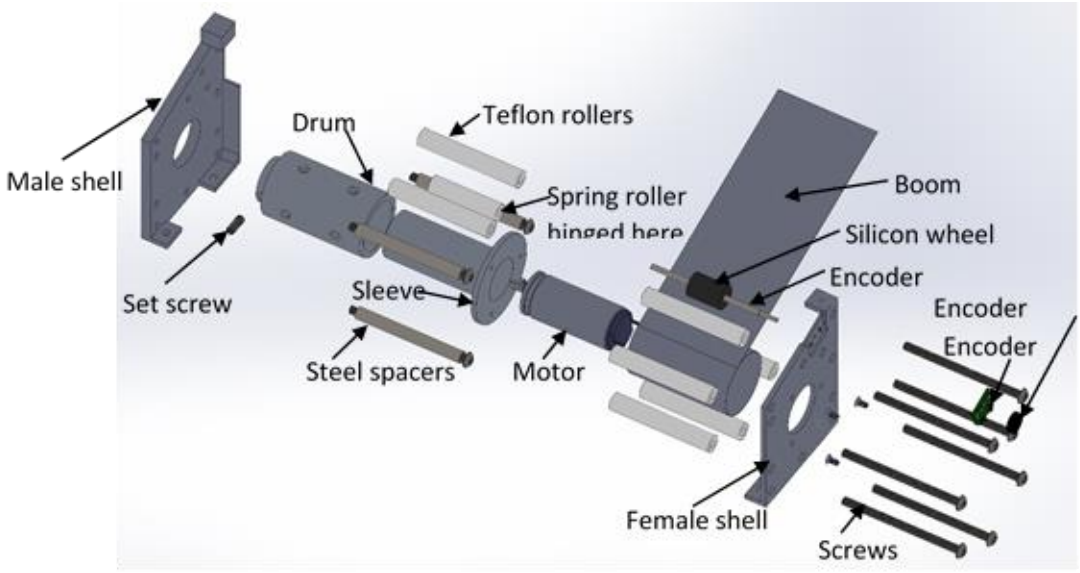

Figure 2. DMD Deployer Expanded View

will then work to passively align this axis with the nadir or zenith vector. Running the B-Dot de-tumble law [7] using magnetorquers embedded in the DMD serves to damp initial satellite rotation rates and the attitude oscillations that will persist after boom deployment. The combination of aerodynamic, gravity gradient, and magnetic torques generated by the DMD provide 3-axis attitude stabilization and ensure that a single face of the satellite is pointing toward Earth with negligible power usage after the initial detumble and stabilization. As a bonus, the DMD booms can be collectively deployed or retracted to vary the cumulative aerodynamic drag experienced by the satellite which can be utilized for orbital maneuvering, constellation phasing, collision avoidance, and controlled re-entry [11]. Each DMD deployer (Figure 2) contains a brushed DC motor (Faulhaber 1516-006SR with 262:1 spur gearbox) that drives a drum to which the boom is connected. As the motor rotates, the boom deploys and drives a rotary encoder that precisely measures the amount of boom deployment.

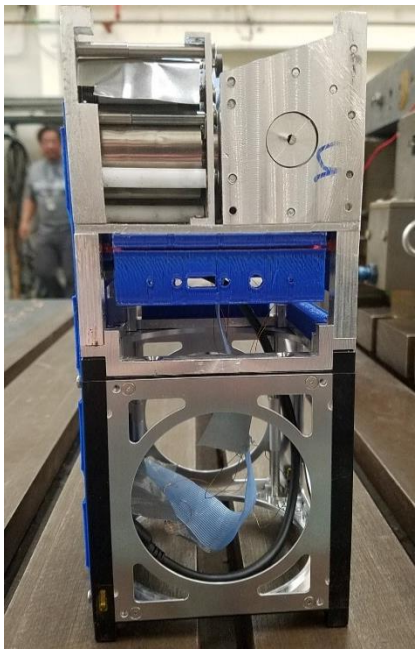

Figure 3. Prototype of DMD with CubeSat Structure

The DMD attaches to a host CubeSat via a structural interface adapter that also contains the magnetorquers wrapped around 3D printed Ultem brackets, increasing its size by 1U and increases the drag area by up to .5 m^2. DMD mass is approximately 1.3 kg. Figure 3 shows a DMD prototype attached to a 1U CubeSat structure to make a 2U CubeSat form factor.

3. ATTITUDE AND ORBIT SIMULATION FRAMEWORK

To simulate the attitude and orbital dynamics of the satellite, a 6 degree of freedom numerical attitude and orbit propagator was created. The satellite state vector was $\boldsymbol{x} = [\boldsymbol{r^T} \quad \boldsymbol{v^T} \quad \boldsymbol{q^T} \quad \boldsymbol{\omega^T}]^T$ where $\boldsymbol{r}$ is the satellite position vector in the ECI (Earth Centered Inertial) frame, $\boldsymbol{v}$ is the ECI velocity vector, $\boldsymbol{\omega}$ is the angular velocity of the satellite body frame with respect to the ECI frame, and $\boldsymbol{q}$ is the quaternion defining the rotation from the ECI frame to the satellite body frame. $\boldsymbol{q}$ is defined as [12]

$$\boldsymbol{q} = \begin{bmatrix} \hat{\boldsymbol{e}} \sin(\theta/2) \\ \cos(\theta/2) \end{bmatrix} = [q_1 \quad q_2 \quad q_3 \quad q_4]^T \tag{1}$$

Such that a rotation of the ECI frame by angle θ about axis $\hat{\boldsymbol{e}}$ would align it with the spacecraft body frame. At each time step the state derivative is computed and numerically integrated using the RK78 numerical integration method [13].

$$\dot{\boldsymbol{x}} = [\boldsymbol{v^T} \quad \dot{\boldsymbol{v}}^{\boldsymbol{T}} \quad \dot{\boldsymbol{q}}^{\boldsymbol{T}} \quad \dot{\boldsymbol{\omega}}^{\boldsymbol{T}}]^T \tag{2}$$

Where [12]

$$\dot{\boldsymbol{q}} = \frac{1}{2}\begin{bmatrix} q_4 & -q_3 & q_2 & q_1 \\ q_3 & q_4 & -q_1 & q_2 \\ -q_2 & q_1 & q_4 & q_3 \\ -q_1 & -q_2 & -q_3 & q_4 \end{bmatrix}\begin{bmatrix} \omega_x \\ \omega_y \\ \omega_z \\ 0 \end{bmatrix} \tag{3}$$

$$\dot{\boldsymbol{\omega}} = \boldsymbol{I^{-1}}\left(\boldsymbol{T_{net}} - \boldsymbol{\omega} \times (\boldsymbol{I\omega})\right) \tag{4}$$

$$\dot{\boldsymbol{v}} = \frac{\boldsymbol{F_{net}}}{m} \tag{5}$$

Where $\boldsymbol{I}$ is the satellite moment of inertia about the center of mass, $\boldsymbol{T_{net}}$ is the net torque, $\boldsymbol{F_{net}}$ is the net force, and m is the satellite mass. The effects of Earth's non-uniform gravitational field on the orbit are modeled using the EMG2008 gravitational model with spherical harmonics through degree and order ten [14]. The gravitational force including the most significant perturbation (J_2) can be computed by [15]

$$\boldsymbol{F_g} = -\frac{\mu_e}{r^3}\boldsymbol{r} + \left(\frac{3J_2\mu_e R_e^2}{2r^5}\begin{bmatrix} r_x(5r_z^2/r^2 - 1) \\ r_y(5r_z^2/r^2 - 1) \\ r_z(5r_z^2/r^2 - 3) \end{bmatrix}\right) \tag{6}$$

Where R_e is the equatorial radius of the Earth, μ_e is earth's gravitational parameter, and J_2 is a constant related to the oblateness of the Earth. To compute the aerodynamic drag force and torque acting on the spacecraft, the satellite is discretized into a collection of rectangular panels. The aerodynamic force acting at the centroid of each panel is calculated by

$$\boldsymbol{F_p} = -\frac{1}{2}C_d A \rho v_\perp \boldsymbol{v}_\perp \tag{7}$$

Where C_d is the drag coefficient, ρ is ambient density, A is the surface area of the panel, and $\boldsymbol{v}_\perp$ is the projection of the velocity vector relative to the atmosphere ($\boldsymbol{v}_\infty$) along the panel normal vector $\hat{\boldsymbol{n}}_{\boldsymbol{p}}$. If $\boldsymbol{v}_\infty$ and $\hat{\boldsymbol{n}}_{\boldsymbol{p}}$ are more than 90 degrees apart, the panel does not experience any drag force and $\boldsymbol{v}_\perp$ is set to zero. $\boldsymbol{v}_\infty$ and $\boldsymbol{v}_\perp$ are computed by

$$\boldsymbol{v}_\infty = \boldsymbol{v} - \boldsymbol{\omega_e} \times \boldsymbol{r} \tag{8}$$

$$\boldsymbol{v}_\perp = \max(\boldsymbol{v}_\infty \cdot \hat{\boldsymbol{n}}_{\boldsymbol{p}}, 0) \tag{9}$$

Where $\boldsymbol{\omega_e}$ is the rotation rate of the Earth. If $\boldsymbol{r_p}$ is the vector from the satellite center of mass to the panel centroid, the aerodynamic torque resulting from the panel is

$$\boldsymbol{\tau_p} = \boldsymbol{r_p} \times \boldsymbol{F_p} \tag{10}$$

The aerodynamic forces and torques generated by each panel are summed to get the net aerodynamic force and torque. The spacecraft's attitude, position, and moment of inertia tensor are utilized to compute the gravity gradient torques with Eq. 3.155 in [2].

$$\boldsymbol{\tau_{gg}} = \frac{3\mu_e}{r^3}\hat{\boldsymbol{n}} \times (\boldsymbol{J}\hat{\boldsymbol{n}}) \tag{11}$$

Where r is the distance from the center of the Earth to the satellite center of mass, $\hat{\boldsymbol{n}}$ is the nadir vector expressed in the spacecraft body frame, and $\boldsymbol{J}$ is the satellite moment of inertia tensor about the center of mass. Finally, the magnetic torques acting on the satellite are given by [2]

$$\boldsymbol{\tau_{mag}} = \boldsymbol{\mu} \times \boldsymbol{B} \tag{12}$$

Where $\boldsymbol{\mu}$ is the spacecraft magnetic moment vector and $\boldsymbol{B}$ is the Earth's magnetic field vector.

4. CONTROL METHODOLOGY

The satellite will begin in a tumbling state after deployment into space with the DMD booms retracted. At this point, the BDot de-tumble controller will be activated and the magnetorquers will be used to set the spacecraft magnetic moment to [16]

$$\boldsymbol{\mu_{bdot}} = -K\dot{\hat{\boldsymbol{B}}} = -K\left(\hat{\boldsymbol{B}} \times \boldsymbol{\omega}\right) \approx -K\frac{\hat{\boldsymbol{B}}_2 - \hat{\boldsymbol{B}}_1}{\Delta t} \tag{13}$$

Where K is a user defined, positive gain and $\hat{\dot{\boldsymbol{B}}}$ is the rate of change of the unit Earth magnetic field vector in the spacecraft body frame as measured by a magnetometer. As shown in Figure 4, this ensures that the direction of the resulting magnetic torque vector given by Eq. (12) will be as close as possible to $-\boldsymbol{\omega}$ and thus will reduce spacecraft angular velocity to the extent possible. This can be proven more formally as follows.

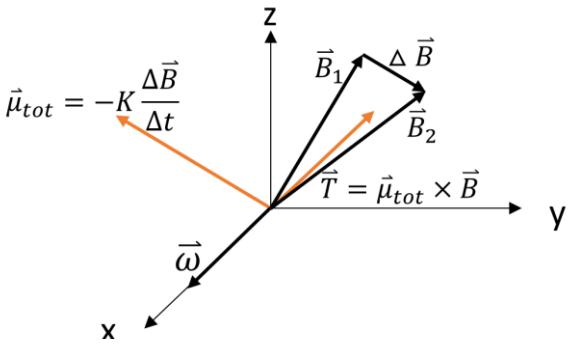

Figure 4. BDot Detumble Controller

Substituting Eq. (13) into Eq. (12) gives the magnetic torque vector from the BDot law

$$\boldsymbol{\tau_{bdot}} = -K\left(\hat{\boldsymbol{B}} \times \boldsymbol{\omega}\right) \times \boldsymbol{B} \tag{14}$$

The triple vector product rule states that for any three vectors $\boldsymbol{A}, \boldsymbol{B}$, and $\boldsymbol{C}$ [17]

$$(\boldsymbol{A} \times \boldsymbol{B}) \times \boldsymbol{C} = -\boldsymbol{A}(\boldsymbol{B} \cdot \boldsymbol{C}) + \boldsymbol{B}(\boldsymbol{A} \cdot \boldsymbol{C}) \tag{15}$$

Applying this to Eq. (14) yields

$$\boldsymbol{\tau_{bdot}} = K\hat{\boldsymbol{B}}\left(\omega B\cos(\theta)\right) - K\boldsymbol{\omega}B \tag{16}$$

Where θ is the angle between $\boldsymbol{\omega}$ and $\boldsymbol{B}$. Taking the dot product of Eq. (16) and $\hat{\boldsymbol{\omega}}$ gives the component of $\boldsymbol{\tau_{bdot}}$ along the $\boldsymbol{\omega}$ direction. If this component is negative, then $\boldsymbol{\omega}$ will be reduced in magnitude.

$$\begin{aligned} \boldsymbol{\tau_{bdot}} \cdot \boldsymbol{\omega} &= K\cos(\theta)\left(\omega B\cos(\theta)\right) - K\omega B \\ &= -KB\omega(1 - \cos^2(\theta)) \leq 0 \end{aligned} \tag{17}$$

Eq. (17) will be less than zero in all cases except for when θ equals zero. This occurs when the magnetic field is aligned with angular velocity vector and will result in zero magnetic torque (no reduction in angular velocity). However, because the direction of the magnetic field vector changes along the orbit, a condition with $\theta = 0$ will not persist for any significant time. This ensures that the BDot law will be able to reliably reduce the angular velocity of the satellite.

In addition to $\boldsymbol{\mu_{bdot}}$, a fixed magnetic moment vector along the desired zenith-pointing satellite axis (in this case the x-axis in Figure 1), will be superimposed on $\boldsymbol{\mu_{bdot}}$ after de-tumble and partial boom deployment. This fixed magnetic moment will work to align the x-axis with the Earth's magnetic field. At the point in the orbit when the magnetic field (and hence the satellite x-axis) is most-zenith pointing (as determined in advance through orbit propagation), the two DMD booms along the x-axis will be fully deployed and the two booms along the y-axis will be partially deployed. This creates a minimum moment of inertia about the x-axis which gravity gradient torques will naturally align with the zenith vector. Aerodynamic torques will simultaneously align the DMD z-axis (Figure 1) with the velocity vector, resulting in passive 3-axis attitude stabilization. All booms can be simultaneously deployed or retracted to facilitate orbital maneuvering while maintaining this attitude stability.

5. SIMULATIONS RESULTS

Figure 5 displays the attitude in the Local-Vertical-Local-Horizontal (LVLH) [3] frame of a 2U, DMD-equipped CubeSat initially deployed from the International Space Station (circular orbit with inclination of 52 degrees and semi major axis of 6778 *km*). Note that the LVLH x-axis is aligned with the zenith vector and the z-axis is aligned with the orbit angular momentum vector. In the first 10,000 seconds of the simulation, only the B-Dot

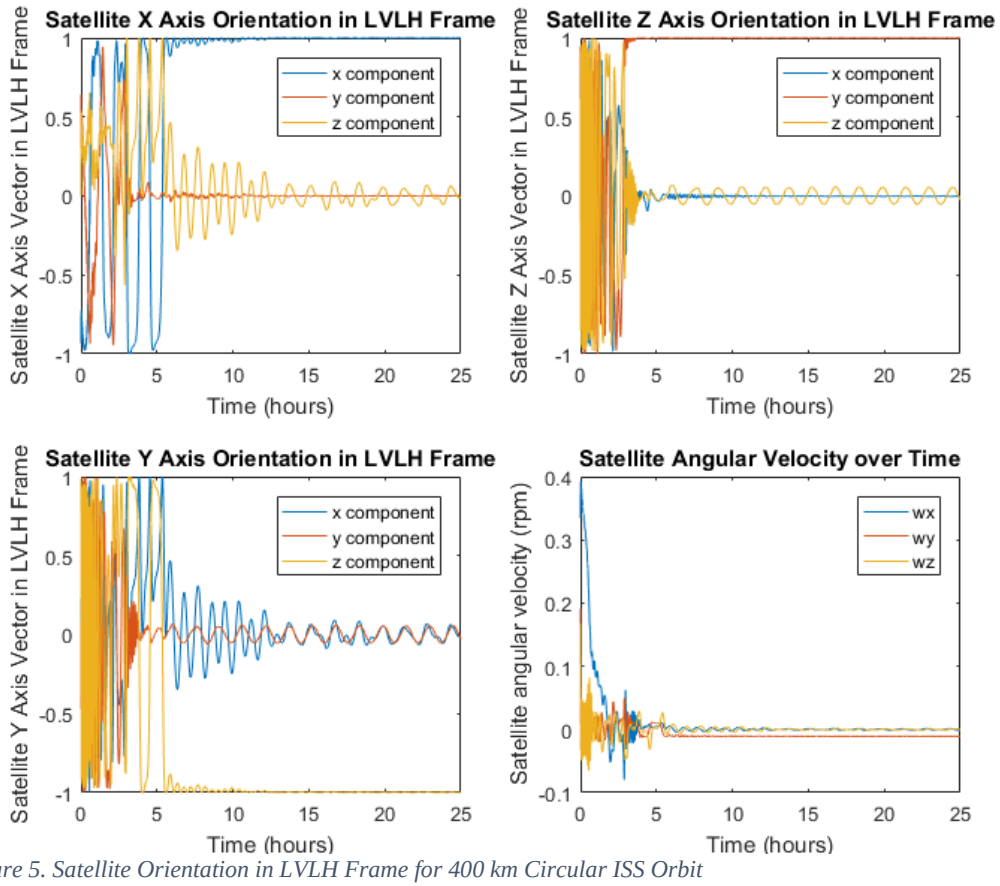

Figure 5. Satellite Orientation in LVLH Frame for 400 km Circular ISS Orbit

controller is run (retracted booms) with a BDot gain of -5 to de-tumble the satellite. Between t=10,000 and t=20,000 seconds, all booms are deployed to 1 m and a fixed magnetic moment of .015 $A*m^2$ along the satellite body frame x-axis is superimposed on the B-Dot magnetic moment. The $+y$ and $-y$ booms are then deployed to 1.85 m and the $+x$ and $-x$ booms are deployed to 3.7 m at the point in the next orbit when the magnetic field is most zenith pointing (t=20,800 s). After this, the fixed magnetic moment is removed and only the B-Dot controller continues running to damp attitude oscillations. Note that the attitude oscillations are never completely removed due to the movement of the zenith and velocity vectors in inertial space over the course of each orbit. The satellite eventually stabilizes with the z-axis aligned with the velocity vector and the x-axis aligned with the zenith vector with a steady state pointing error of less than five degrees. Figure 6 shows the error angle between the actual and desired orientation over time.

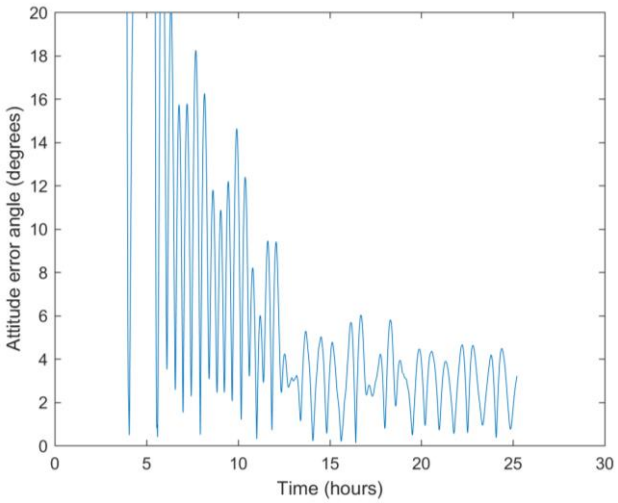

Figure 6. Angle Between Actual and Desired Attitude over Time

6. CONCLUSIONS

The drag maneuvering device is a unique actuator capable of providing simultaneous orbital maneuvering capabilities and semi-passive attitude stabilization. By independently actuating four tape-spring booms, the DMD can leverage naturally occurring aerodynamic and gravity gradient torques for attitude stability. Embedded magnetorquers are actuated based on magnetometer measurements to damp attitude oscillations and to ensure gravity gradient stabilization in the proper orientation. A control methodology for the DMD is developed in this paper and numerical attitude and orbit simulations verify the capabilities of the DMD. For many Low Earth Orbit satellite missions, particularly for Earth observation, the DMD could be used to entirely replace conventional attitude control and propulsion systems. For example, the DMD could maintain a camera or antenna pointed at the Earth while modulating aerodynamic drag to maintain an orbit slot.

7. REFERENCES

[1] R. E. Roberson, "Two Decades of Spacecraft Attitude Control," *Journal of Guidance, Control, and Dynamics*, vol. 2, no. 1, pp. 3–8, 1979.

[2] F. L. Markley and J. L. Crassidis, *Fundamentals of Spacecraft Attitude Determination and Control*. New York: Springer-Verlag, 2014.

[3] H. Curtis, *Orbital Mechanics for Engineering Students*, 2nd ed. Burlington, MA: Elsevier, 2009.

[4] S. K. Shrivastava and V. J. Modi, "Satellite attitude dynamics and control in the presence of environmental torques - A brief survey," *Journal of Guidance, Control, and Dynamics*, vol. 6, no. 6, pp. 461–471, Nov. 1983.

[5] H. Heidt, J. Puig-Suari, A. Moore, S. Nakasuka, and R. Twiggs, "CubeSat: A New Generation of Picosatellite for Education and Industry Low-Cost Space Experimentation," in *Proceedings of the 14th Annual AIAA/USU Conference on Small Satellites*, Logan, UT, 2000.

[6] M. Pastorelli, R. Bevilacqua, and S. Pastorelli, "Differential-Drag-based Roto-Translational Control for Propellant-less Spacecraft," *Acta Astronautica*, vol. 114, pp. 6–21, Sep. 2015.

[7] C. Arduini and P. Baiocco, "Active Magnetic Damping Attitude Control for Gravity Gradient Stabilized Spacecraft," *Journal of Guidance, Control, and Dynamics*, vol. 20, no. 1, pp. 117–122, 1997.

[8] E. Silani and M. Lovera, "Magnetic spacecraft attitude control: a survey and some new results," *Control Engineering Practice*, vol. 13, no. 3, pp. 357–371, Mar. 2005.

[9] R. R. Kumar, D. D. Mazanek, and M. L. Heck, "Simulation and Shuttle Hitchhiker validation of passive satellite aerostabilization," *Journal of Spacecraft and Rockets*, vol. 32, no. 5, pp. 806–811, Sep. 1995.

[10] D. Guglielmo *et al.*, "Drag Deorbit Device: A New Standard Reentry Actuator for CubeSats," *AIAA Journal of Spacecraft and Rockets*, vol. 56, no. 1, pp. 129–145, 2019.

[11] S. Omar and R. Bevilacqua, "Guidance, Navigation, and Control Solutions for Spacecraft Re-Entry Point Targeting using Aerodynamic Drag," *Acta Astronautica*, 2018.

[12] B. Wie, *Space Vehicle Dynamics and Control, Second Edition*. Reston ,VA: American Institute of Aeronautics and Astronautics, 2008.

[13] O. Montenbruck and E. Gill, *Satellite Orbits*, 1st ed. Springer Berlin Heidelberg, 2005.

[14] N. K. Pavlis, S. A. Holmes, S. C. Kenyon, and J. K. Factor, "An Earth Gravitation Model to Degree 2160: EGM2008," presented at the 2008 General Assembly of European Geosciences Union, Vienna, Austria, 03-Apr-2008.

[15] R. R. Bate, D. D. Mueller, and J. E. White, *Fundamentals of astrodynamics*. New York: Dover Publications, 1971.

[16] A. C. Stickler and K. t. Alfriend, "Elementary Magnetic Attitude Control System," *Journal of Spacecraft and Rockets*, vol. 13, no. 5, pp. 282–287, May 1976.

[17] G. Arfken, "Triple Scalar Product, Triple Vector Product," in *Mathematical Methods for Physicists*, 3rd ed., Orlando, FL: Academic Press, 1985, pp. 26–33.